

MIXED FORMULATION OF NONLINEAR STEEL-CONCRETE COMPOSITE BEAM ELEMENT

By Ashraf Ayoub,¹ Associate Member, ASCE, and Filip C. Filippou,² Member, ASCE

ABSTRACT: This paper presents an inelastic beam element for the analysis of steel-concrete girders with partial composite action under monotonic and cyclic loads. The element is derived from a two-field mixed formulation with independent approximation of internal forces and transverse displacements. The nonlinear response of the steel and concrete component of the girder is based on the section discretization into fibers with uniaxial hysteretic material models for the constituent materials. The partial interaction between concrete deck and steel girder through shear connectors is accounted for by an interface model with distributed force transfer characteristics. A direct state determination algorithm for the implementation of the composite element in a general purpose nonlinear analysis program is presented, and the stability characteristics of the algorithm are discussed in conjunction with the selection of appropriate force and displacement interpolation functions. The validity of the model is established by correlation of analytical results with experimental evidence. Numerical studies are used to compare the model with the classical displacement formulation. These studies confirm the superiority of the proposed model in modeling composite girders under monotonic and cyclic loads that induce stiffness deterioration and strength softening.

INTRODUCTION

Composite steel-concrete construction is widely used in buildings and bridges, even in regions of high seismic risk (Viest et al. 1997). This fact stems from economic and structural benefits that accrue from the combination of the advantages of structural steel (speed of construction) with those of concrete (stiffness) and the elimination of shortcomings of the constituent materials through careful design of structural components. The increased use of this type of construction in regions of high seismic risk recently led to a concerted research effort within the framework of the U.S.-Japan program. In composite girders the mechanical bond between concrete deck and steel girder through deformable shear connectors induces the concrete slab to act as an integral part of the beam and leads to an increase in strength and stiffness of the composite girder. By proper selection of the strength, stiffness, and spacing of connectors, full or partial composite action can be achieved [Eurocode 4 ("Design" 1992) and LRFD specification]. Several researchers have pursued the effect of partial composite action in the analysis of composite girders in the linear elastic case. Few studies have, however, so far addressed the nonlinear response of composite girders, particularly, with regard to the nonlinear behavior of shear connectors, and the behavior under cyclic loads.

Timoshenko (1925) developed a theory for composite beams with two bonded materials using Bernoulli-Euler beam theory for each component and constraining transverse displacements to be equal. Newmark et al. (1951) established the governing equations for elastically connected steel-concrete beams neglecting uplift and friction. Adekola (1968) extended this work by including uplift and frictional effects. He proposed a finite-difference procedure for solving the differential equation for uplift and axial forces. Robinsion and Naraine (1988) addressed the issue of whether the forces at the interface act on the concrete slab or pull on the steel beam. Cosenza

and Mazzolani (1993) proposed a new solution procedure that is suitable for general loading conditions and McGarraugh and Baldwin (1971) used a simple analytical model to prove that the strength of a composite girder with partial interaction can be derived by nonlinear interpolation of the beam strength for the extreme cases of no interaction and full interaction.

For the study of the nonlinear behavior of composite members the existing studies can be grouped into the following two categories: (1) Finite-element models utilizing beam, plate, shell, or brick finite elements to represent in great detail the constituents of the composite structural element (such models are rather complex, very computationally intensive, and limited to monotonic loads); and (2) 1D beam elements that capture salient features of the nonlinear behavior of composite girders within the framework of Navier-Bernoulli beam theory. Within the latter category proposed models can be grouped into three categories: (1) Full composite action models based on displacement interpolation functions with fiber discretization of the cross section and uniaxial stress-strain relations of the constituent materials, as proposed by Mirza and Skrabek (1991) for the analysis of composite columns under uniaxial bending and El-Tawil et al. (1995) under biaxial bending; (2) models of the partial composite action between concrete and steel based on displacement interpolation functions for the concrete and steel component of the composite element, which readily supply the relative longitudinal or transverse displacement at the interface; in this category belong the study by Daniel and Crisinel (1993) for composite beams under monotonic loads, the study by Amadio and Fragiaco (1993) for the effect of concrete creep and shrinkage in composite beams, the study by Hajjar et al. (1997) for concrete-filled, steel tube columns, and the study by Salari et al. (1997) for composite beams under cyclic loads; and (3) recent models that attempt to overcome the limitations of displacement-based models by the use of force interpolation functions (flexibility formulation); interest in this type of nonlinear model increased after the work by Ciampi and Carlesimo (1986), who are the first to propose a consistent implementation of the flexibility formulation of a nonlinear Bernoulli beam element within the framework of a general purpose nonlinear analysis program. The selection of suitable force interpolation functions that strictly satisfy equilibrium is rather straightforward for the case of a nonlinear Bernoulli beam element; in this case the fiber discretization of the cross section affords a convenient means of describing the complex hysteretic response of members under cyclic loading histories (Spacone et al. 1996b). Difficulties arise, however, in the selection of force interpolation

¹Postdoctoral Res. Fellow, Stanford Univ., Stanford, CA 94305; formerly, Doctoral Student, Univ. of California, Berkeley, Berkeley, CA 94720-1710.

²Prof., Dept. of Civ. and Envir. Engrg., Univ. of California, Berkeley, Berkeley, CA.

Note. Associate Editor: Bill Spencer. Discussion open until August 1, 2000. To extend the closing date one month, a written request must be filed with the ASCE Manager of Journals. The manuscript for this paper was submitted for review and possible publication on April 28, 1999. This paper is part of the *Journal of Structural Engineering*, Vol. 126, No. 3, March, 2000. ©ASCE, ISSN 0733-9445/00/0003-0371-0381/\$8.00 + \$.50 per page. Paper No. 20764.

functions that strictly satisfy equilibrium for cases that involve interaction between beam displacements and internal forces. Examples are an anchored reinforcing bar, a prestressed concrete girder, a steel-concrete girder with partial composite action, and a slender column. Attempts to extend the advantages of a force-based flexibility formulation to these cases have been recently reported (Yassin 1994; Ayoub and Filippou 1997; Monti et al. 1997; Neuenhofer and Filippou 1998; Salari et al. 1998). With the exception of the study by Neuenhofer and Filippou (1998), which is, however, limited to linear elastic material behavior, the other studies resort to ad hoc assumptions for overcoming the difficulty of deriving force interpolation functions that strictly satisfy equilibrium. The formulations by Yassin (1994), Monti et al. (1997), and Ayoub and Filippou (1997) limit the interaction between the two components to the end nodes of the element and assume a linear interpolation of bond or friction forces in between. This requires a small element size for accurate local response eliminating one of the advantages of the flexibility-based formulation (Neuenhofer and Filippou 1997). To overcome this weakness Salari et al. (1998) introduced higher order bond force distribution functions. The formulation, however, lacks clarity about the relation between the slip distribution in the element and the element end displacements. Analytical results reveal interelement discontinuities of slip displacements in violation of variational principles. It is also not clear that the element can be extended to accommodate distributed element loads.

In view of the limitations of the displacement formulation (Neuenhofer and Filippou 1997) and the difficulty of selecting force interpolation functions that strictly satisfy equilibrium for problems with strong interaction between displacements and internal forces, Ayoub and Filippou (1999) recently proposed a consistent mixed formulation of the anchored reinforcing bar problem with independent interpolation functions for the axial displacements and the reinforcing steel stresses. This formulation combines the advantages of the displacement and force formulations while overcoming most of their limitations. This paper extends the consistent framework of the mixed formulation to the more complex problem of a girder with partial composite action.

GOVERNING EQUATIONS FOR COMPOSITE BEAM ELEMENT

Equilibrium

Fig. 1 shows a composite beam with the concrete deck on top of the steel girder and an infinitesimal portion with the internal forces and applied element loads. Force variables referring to concrete are denoted by subscript *c* and those referring to steel by subscript *s*. The equations of equilibrium for each component of the beam including slip and uplift effects are derived with Adekola's approach (1968) as follows.

Concrete deck element:

$$\frac{dN_c}{dx} - t_b = 0; \quad \frac{dV_c}{dx} + (w_t + t_t) = 0; \quad \frac{dM_c}{dx} + V_c - h_1 t_b = 0 \quad (1a)$$

Steel girder element:

$$\frac{dN_s}{dx} + t_b = 0; \quad \frac{dV_s}{dx} - t_t = 0; \quad \frac{dM_s}{dx} + V_s - h_2 t_b = 0 \quad (1b)$$

where *N*, *V*, and *M* denote the axial force, shear force, and bending moment, respectively; *t_b* = longitudinal force; *t_t* = transverse force per unit length at the interface of the concrete deck with the steel girder; *w_t* denotes the distributed load on

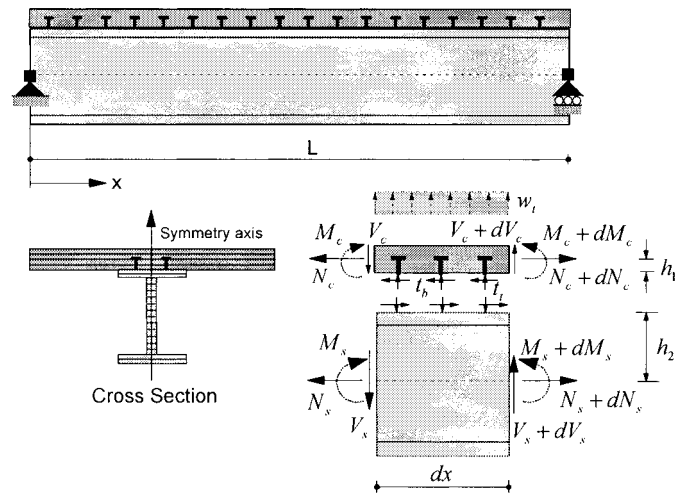


FIG. 1. Composite Beam with Segment Equilibrium

the girder, which is assumed to act on the concrete deck; *h₁* = distance between a reference point of the concrete deck and the interface; and *h₂* = distance between a reference point of the steel girder and the interface. It is customary to select the geometric centroid of the corresponding component as the reference point, but any other point can be used as well. All terms in (1) are functions of *x*, except for *h₁* and *h₂* which are assumed constant. Tapered beams can thus be handled only by subdivision of the girder into elements of uniform depth. The elimination of the shear force from the flexure equilibrium equations in (1) yields

$$\frac{d^2 M_c}{dx^2} - (w_t + t_t) - h_1 \frac{dt_b}{dx} = 0; \quad \frac{d^2 M_s}{dx^2} + t_t - h_2 \frac{dt_b}{dx} = 0 \quad (2a,b)$$

The addition of the equations in (2) results in

$$\frac{d^2 M}{dx^2} - w_t - h \frac{dt_b}{dx} = 0 \quad (3)$$

where *M* = *M_s* + *M_c* = sum of the moments resisted by the steel and concrete component; and *h* = *h₁* + *h₂* = distance between the reference axes of the two components. With (3) and the axial equilibrium equations from (1), the governing equilibrium equations for the composite girder can be summarized as follows:

$$\frac{dN_c}{dx} - t_b = 0; \quad \frac{dN_s}{dx} + t_b = 0 \quad (4a,b)$$

$$\frac{d^2 M}{dx^2} - w_t - h \frac{dt_b}{dx} = 0 \quad (4c)$$

The total moment resisted by the composite section *d²M/dx²* - *h(dt_b/dx)* can be directly obtained from the solution of the last equilibrium equation in [(4c)]. Thus, force interpolation functions for the total moment can be readily established and satisfy equilibrium in a strict sense.

Eq. (4) can be written in compact form

$$\begin{bmatrix} \frac{d}{dx} & 0 & 0 & -1 \\ 0 & \frac{d}{dx} & 0 & 1 \\ 0 & 0 & \frac{d^2}{dx^2} & -h \frac{d}{dx} \end{bmatrix} \begin{pmatrix} N_c \\ N_s \\ M \\ t_b \end{pmatrix} - \begin{pmatrix} 0 \\ 0 \\ w_t \end{pmatrix} = \begin{pmatrix} 0 \\ 0 \\ 0 \end{pmatrix}$$

$$\text{or } \tilde{\mathbf{L}}^T \tilde{\mathbf{s}}(x) - \mathbf{w} = \mathbf{0} \quad (5)$$

where $\tilde{\mathbf{s}}(x)$ = internal force vector; $\tilde{\mathbf{L}}$ = differential operator; and \mathbf{w} = vector of applied element loads. It is expedient for the subsequent finite-element formulation to split the internal force vector $\tilde{\mathbf{s}}(x)$ in two parts: (1) a vector $\mathbf{s}(x)$, which contains N_c , N_s , and M ; and (2) a scalar $s_b(x)$, which represents the longitudinal shear force at the interface $t_b(x)$. With this change (5) becomes

$$\mathbf{L}^T \mathbf{s}(x) - \mathbf{L}_b^T s_b(x) - \mathbf{w} = \mathbf{0} \quad (6)$$

where \mathbf{L} = diagonal differential operator.

$$\mathbf{L} = \begin{bmatrix} \frac{d}{dx} & 0 & 0 \\ 0 & \frac{d}{dx} & 0 \\ 0 & 0 & \frac{d^2}{dx^2} \end{bmatrix} \quad (7)$$

and $\mathbf{L}_b = [1 \quad -1 \quad h(d/dx)]$.

Compatibility

The congruent deformation measures to the internal forces $\mathbf{s}(x)$ are the axial strain ϵ_c at the reference axis of the concrete deck, the axial strain ϵ_s at the reference axis of the steel girder, and the curvature κ of the composite section. The deformation vector is denoted by $\mathbf{e}(x)$ where

$$\mathbf{e}(x) = \begin{pmatrix} \epsilon_c \\ \epsilon_s \\ \kappa \end{pmatrix} \quad (8)$$

The relative displacement between concrete deck and steel girder is denoted by e_b and is congruent to the shear force s_b at the interface.

The compatibility conditions establish the relation between the displacements of the composite girder and the deformation measures. Neglecting the relative transverse displacement between the concrete deck and the steel girder yields the following compatibility relations:

$$\frac{du_{1c}}{dx} - \epsilon_c = 0; \quad \frac{du_{1s}}{dx} - \epsilon_s = 0; \quad \frac{d^2 u_2}{dx^2} - \kappa = 0 \quad (9a-c)$$

$$\left(u_{1c} + h_1 \frac{du_2}{dx} \right) - \left(u_{1s} - h_2 \frac{du_2}{dx} \right) - e_b = 0 \quad (9d)$$

where u_{1s} = axial displacement at the reference axis of the steel girder; u_{1c} = axial displacement at the reference axis of the concrete deck; and u_2 = transverse displacement of the composite girder.

The compatibility equations in (9) can be written in compact form

$$\begin{bmatrix} \frac{d}{dx} & 0 & 0 \\ 0 & \frac{d}{dx} & 0 \\ 0 & 0 & \frac{d^2}{dx^2} \\ 1 & -1 & h \frac{d}{dx} \end{bmatrix} \begin{pmatrix} u_{1c} \\ u_{1s} \\ u_2 \end{pmatrix} - \begin{pmatrix} \epsilon_c \\ \epsilon_s \\ \kappa \\ e_b \end{pmatrix} = \begin{pmatrix} 0 \\ 0 \\ 0 \\ 0 \end{pmatrix} \quad \text{or} \quad \tilde{\mathbf{L}} \mathbf{u}(x) - \tilde{\mathbf{e}}(x) = \mathbf{0} \quad (10)$$

where $\mathbf{u}(x)$ = displacement vector at x ; and $\tilde{\mathbf{e}}(x)$ = complete deformation vector made up of \mathbf{e} and e_b . The contragradient nature of the differential operator $\tilde{\mathbf{L}}$ in the equilibrium and compatibility equations [(5) and (10)], respectively, confirms

the selection of congruent force and deformation measures for the composite girder. Eq. (10) can be split in two parts

$$\mathbf{L} \mathbf{u}(x) - \mathbf{e}(x) = \mathbf{0}; \quad \mathbf{L}_b \mathbf{u}(x) - e_b(x) = 0 \quad (11a,b)$$

to correspond to the modified form of the equilibrium equations in (6).

Constitutive Force-Deformation Relations

The internal forces of the composite girder \mathbf{s} are related to the deformation measures \mathbf{e} by a nonlinear constitutive relation

$$\mathbf{s}(x) = \hat{\mathbf{g}}(\mathbf{e}(x)) \quad (12)$$

In this study the nonlinear relation in (12) is derived from a layer discretization of the cross section of the composite girder with nonlinear, uniaxial stress-strain relations for the constituent materials (Fig. 1). Such a model directly accounts for the interaction between axial force and bending moment. The uniaxial concrete stress-strain relation follows the model by Scott et al. (1982) with a cyclic degradation of the unloading-reloading stiffness according to the proposal by Karsan and Jirsa (1969). A typical hysteretic response is shown in Fig. 2(a). The uniaxial steel stress-strain relation follows the model of Menegotto and Pinto (1973) with kinematic and isotropic hardening. A typical hysteretic response is shown in Fig. 2(b). More details are provided elsewhere (Filippou et al. 1983). The shear force s_b at the interface between steel girder and concrete deck is related to the relative slip e_b by a nonlinear relation of the form

$$s_b = \hat{g}_b(e_b) \quad (13)$$

The shear force-slip relation at the interface of the steel girder with the concrete deck is described by a model similar to that proposed by Eigenhausen et al. (1983) for the bond stress-slip relation of anchored reinforcing bars. A typical hysteretic response of the model is compared with experimental evidence from push-pull connector specimens by Bursi and Ballerini (1996) in Figs. 2(c and d).

MIXED FORMULATION OF COMPOSITE BEAM ELEMENT

In the mixed finite-element formulation the governing equations of the problem in (6) and (11)–(13) are not reduced to a single force or displacement field as is the case in the displacement or force formulation. Instead, two or more independent fields are used, so that several variations are possible (Zienkiewicz and Taylor 1991): $\mathbf{u}(x)$ - $\mathbf{s}(x)$ field approximation, $\mathbf{u}(x)$ - $\mathbf{e}(x)$ - $\mathbf{s}(x)$ field approximation, and $\mathbf{u}(x)$ - $\mathbf{e}(x)$ - $s_b(x)$ field approximation. The first option is selected in this study on account of the smooth variation of element displacements and internal forces. By contrast, the section deformations $\mathbf{e}(x)$ are derivatives of displacements, and the interface shear forces $s_b(x)$ are derivatives of axial forces and vary more abruptly.

In the context of the proposed finite-element solution for (6) and (11)–(13) the solution domain is subdivided into discrete elements. On account of the nonlinear character of the material relations in (12) and (13), consistent linearization of the governing equations for a single element is used to derive the incremental force-deformation relation of the element. The incremental force-displacement relation of the structure is then assembled from the element contributions following well-established principles of structural analysis. The resulting system of equations is solved by an iterative solution strategy, commonly of the Newton-Raphson type. In this solution approach, loads or displacements are imposed in several steps on the structure; for each step the linearized system of equations of the current state of the structure is solved for the unknown

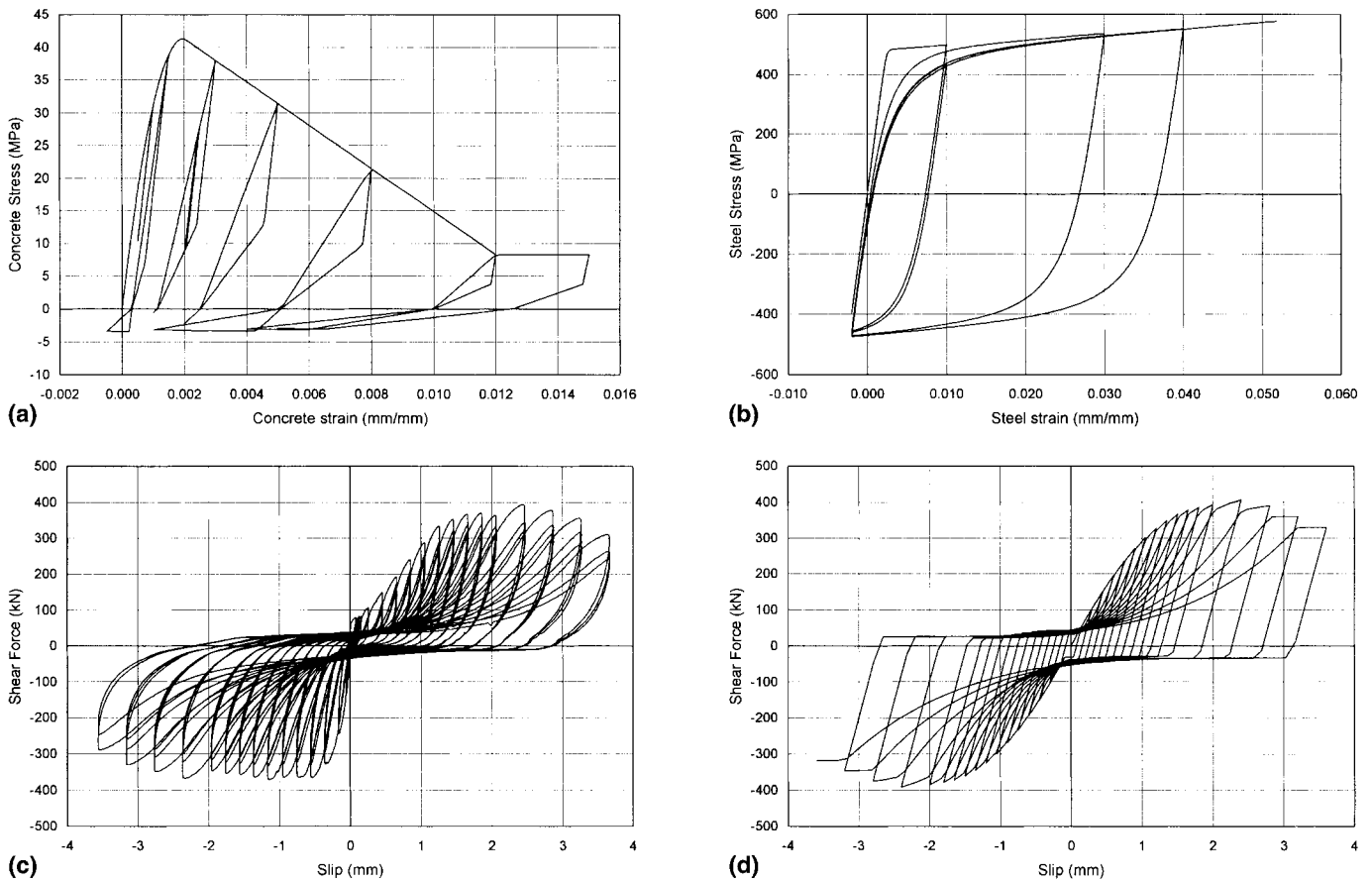


FIG. 2. (a) Hysteretic Stress-Strain Relation for Concrete; (b) Hysteretic Stress-Strain Relation for Structural and Reinforcing Steel; (c) Measured Shear Force-Slip Behavior of Connectors (Bursi and Ballerini 1996); (d) Analytical Model of Shear Force-Slip Behavior of Connectors

increments of the primary variables. The current state is updated by determining the structural stiffness and residual unbalance between imposed and resisting forces, and the process continues with the determination of new increments for the primary variables under the residuals. The iteration continues until convergence is achieved to within a specified tolerance, after which the solution algorithm advances to the next load step. The following derivation refers to a single Newton-Raphson iteration, denoted by superscript i , within a load step of the incremental solution strategy for the governing nonlinear equations.

The composite beam element has 10 displacement degrees of freedom v_1-v_{10} , as shown in Fig. 3(a). These degrees of freedom include the rigid body modes of the element. Three axial degrees of freedom are used in the concrete deck and steel girder, to permit quadratic polynomials for the axial displacements. The remaining four degrees of freedom at the ends of the element uniquely establish the transverse displacements of the composite element with the aid of Hermitian polynomials. The force degrees of freedom are established for a statically determinate basic system. There are six force degrees of freedom q_1-q_6 for the system in Fig. 3(b). Two axial force degrees of freedom are used in the concrete deck and steel girder, to permit a linear variation of the axial force in the two components. A linear variation of total bending moment is established by degrees of freedom q_2 and q_5 , which is the exact solution in the absence of distributed element loads. For higher order displacement or force interpolation functions further internal degrees of freedom can be introduced, so that, in general, there are n_d displacement degrees of freedom and n_s force degrees of freedom. The criteria for the selection of suitable

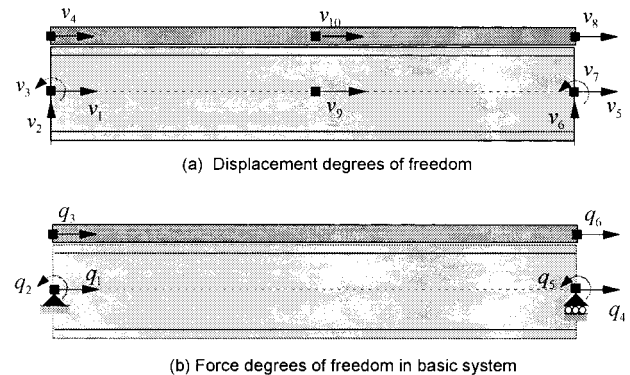


FIG. 3. Degrees of Freedom of Composite Beam Element

force and displacement interpolation functions are discussed in the next section.

The mixed formulation in this paper is based on the integral form of the equilibrium and compatibility equations and follows these steps.

Step 1. The displacement field $\mathbf{u}(x)$ of a typical element is approximated with functions $\mathbf{a}(x)$

$$\mathbf{u}(x) = \mathbf{a}(x)\mathbf{v} \quad (14)$$

where $\mathbf{u}(x) = [u_{1c}(x) \ u_{1s}(x) \ u_2(x)]^T$ = vector of displacements at point x ; and $\mathbf{a}(x) = 3$ by n_d matrix of displacement interpolation functions.

Step 2. The internal force field $\mathbf{s}(x)$ of a typical element is approximated with functions $\mathbf{b}(x)$

$$\mathbf{s}(x) = \mathbf{b}(x)\mathbf{q} \quad (15)$$

where $\mathbf{s}(x) = [N_c(x) \ N_s(x) \ M(x)]^T$ = vector of internal forces at point x ; and $\mathbf{b}(x) = 3$ by n_s matrix of force interpolation functions.

Step 3. The first relation of the mixed formulation derives from the weighted integral form of the compatibility equation at the current element state i and takes the form

$$\int_0^L \delta \mathbf{s}^T(x) [\mathbf{L}\mathbf{u}^i(x) - \mathbf{e}^i(x)] dx = 0 \quad (16)$$

where $\delta \mathbf{s}(x)$ = virtual force field in the role of a weight function and the integration extends over the element length L .

The consistent linearization of the inverse of the force-deformation relation for the composite section in (12) yields

$$\mathbf{e}^i = \mathbf{f}_s^{i-1} \Delta \mathbf{s}^i + \mathbf{e}^{i-1} \quad (17)$$

where \mathbf{e}^{i-1} = section deformation at the end of the last iteration; and \mathbf{f}_s^{i-1} = corresponding composite section flexibility. The inverse form of the constitutive relation is necessary here to ensure symmetry (Zienkiewicz and Taylor 1989). The substitution of (17) into (16) yields

$$\int_0^L \delta \mathbf{s}^T(x) [\mathbf{L}\mathbf{u}^i(x) - \mathbf{f}_s^{i-1} \Delta \mathbf{s}^i - \mathbf{e}^{i-1}] dx = 0 \quad (18)$$

Step 4. With the substitution of the assumed displacement and force interpolation functions from (14) and (15) into (18), and with the use of the same interpolation functions for the corresponding virtual fields according to Galerkin, (18) takes the form

$$\delta \mathbf{q}^T \left\{ \left[\int_0^L \mathbf{b}^T(x) \mathbf{L} \mathbf{a}(x) dx \right] \mathbf{v}^i - \left[\int_0^L \mathbf{b}^T(x) \mathbf{f}_s^{i-1}(x) \mathbf{b}(x) dx \right] \Delta \mathbf{q}^i - \int_0^L \mathbf{b}^T(x) \mathbf{e}^{i-1}(x) dx \right\} = 0 \quad (19)$$

After setting $\mathbf{B}(x) = \mathbf{L} \mathbf{a}(x)$ for the deformation interpolation functions and noting that (19) holds for any $\delta \mathbf{q}$, it follows that

$$\left[\int_0^L \mathbf{b}^T(x) \mathbf{B}(x) dx \right] \mathbf{v}^i - \left[\int_0^L \mathbf{b}^T(x) \mathbf{f}_s^{i-1}(x) \mathbf{b}(x) dx \right] \Delta \mathbf{q}^i - \int_0^L \mathbf{b}^T(x) \mathbf{e}^{i-1}(x) dx = 0 \quad (20)$$

After replacing \mathbf{v}^i by $\mathbf{v}^{i-1} + \Delta \mathbf{v}^i$, (20) becomes

$$\mathbf{T} \Delta \mathbf{v}^i - \mathbf{F}_e^{i-1} \Delta \mathbf{q}^i - \mathbf{v}_r^{i-1} = 0 \quad (21)$$

with

$$\mathbf{T} = \int_0^L \mathbf{b}^T(x) \mathbf{B}(x) dx; \quad \mathbf{F}_e^{i-1} = \int_0^L \mathbf{b}^T(x) \mathbf{f}_s^{i-1}(x) \mathbf{b}(x) dx \quad (22a,b)$$

$$\mathbf{v}_r^{i-1} = \int_0^L \mathbf{b}^T(x) \mathbf{e}^{i-1}(x) dx - \mathbf{T} \mathbf{v}^{i-1} \quad (22c)$$

where \mathbf{F}_e = composite beam flexibility matrix; and \mathbf{v}_r^{i-1} = vector of nodal displacement residuals at the end of the previous iteration. These residuals represent the compatibility error between node displacements \mathbf{v}^{i-1} and deformation field $\mathbf{e}^{i-1}(x)$ before reaching convergence.

Step 5. The weighted integral form of equilibrium (6) at the current element state i takes the form

$$\int_0^L \delta \mathbf{u}^T(x) [\mathbf{L}^T \mathbf{s}^i(x) - \mathbf{L}_b^T s_b^i(x) - \mathbf{w}] ds = 0 \quad (23)$$

where $\delta \mathbf{u}(x)$ = virtual displacement field in the role of a weight function. For the sake of simplicity the effect of element loads \mathbf{w} is not pursued further in this study, and \mathbf{w} is set equal to zero in (23). At this stage in the formulation integration by parts is used to shift the differential operators \mathbf{L} and \mathbf{L}_b from the force fields $\mathbf{s}(x)$ and $s_b(x)$ to the virtual displacement field $\delta \mathbf{u}(x)$. A single integration by parts is necessary for the axial force equations, and two successive integrations are required for the moment equilibrium equation in (23). This process results in several boundary terms that represent the virtual work of virtual node displacements $\delta \mathbf{v}$ with real end forces \mathbf{q} . After changing sign for all terms of the first two equations the process yields

$$\int_0^L \mathbf{L}^T \delta \mathbf{u}^T(x) \mathbf{s}^i(x) dx + \int_0^L \mathbf{L}_b^T \delta \mathbf{u}^T(x) s_b^i(x) dx = \mathbf{B} \mathbf{T} \quad (24)$$

where $\mathbf{B} \mathbf{T}$ = boundary terms. The consistent linearization of the force-slip relation at the interface of the steel girder with the concrete deck in (13) yields

$$s_b^i = k_b^{i-1} \Delta e_b^i + s_b^{i-1} \quad (25)$$

and the substitution of (25) into (24) results in

$$\int_0^L \mathbf{L}^T \delta \mathbf{u}^T(x) \mathbf{s}^i(x) dx + \int_0^L \mathbf{L}_b^T \delta \mathbf{u}^T(x) [k_b^{i-1} \Delta e_b^i + s_b^{i-1}] dx = \mathbf{B} \mathbf{T} \quad (26)$$

Eq. (26) together with (18) forms the basis of the two-field mixed formulation.

Step 6. With the substitution of the assumed displacement and force interpolation functions from (14) and (15) into (26) and with the use of the same interpolation functions for the corresponding virtual fields according to Galerkin, (26) takes the form

$$\delta \mathbf{v}^T \left\{ \left[\int_0^L \mathbf{L}^T \mathbf{a}^T(x) \mathbf{b}(x) dx \right] \mathbf{q}^i + \int_0^L \mathbf{L}_b^T \mathbf{a}^T(x) [k_b^{i-1} \Delta e_b^i + s_b^{i-1}] dx \right\} = \mathbf{B} \mathbf{T} \quad (27)$$

With the use of the second compatibility relation in (11) the last equation becomes

$$\delta \mathbf{v}^T \left\{ \left[\int_0^L \mathbf{L}^T \mathbf{a}^T(x) \mathbf{b}(x) dx \right] \mathbf{q}^i + \left[\int_0^L \mathbf{L}_b^T \mathbf{a}^T(x) k_b^{i-1} \mathbf{L}_b \mathbf{a}(x) dx \right] \Delta \mathbf{v}^i + \int_0^L \mathbf{L}_b^T \mathbf{a}^T(x) s_b^{i-1}(x) dx \right\} = \mathbf{B} \mathbf{T} \quad (28)$$

Noting that $\mathbf{B}(x) = \mathbf{L} \mathbf{a}(x)$ and introducing a similar notation for the relative displacement interpolation at the interface $\mathbf{B}_b(x) = \mathbf{L}_b \mathbf{a}(x)$, (28) simplifies to

$$\delta \mathbf{v}^T \left\{ \left[\int_0^L \mathbf{B}^T(x) \mathbf{b}(x) dx \right] \mathbf{q}^i + \left[\int_0^L \mathbf{B}_b^T(x) k_b^{i-1} \mathbf{B}_b(x) dx \right] \Delta \mathbf{v}^i + \int_0^L \mathbf{B}_b^T(x) s_b^{i-1}(x) dx \right\} = \mathbf{B} \mathbf{T} \quad (29)$$

Using the first relation from (22) in the last equation yields

$$\delta \mathbf{v}^T (\mathbf{T}^T \mathbf{q}^i + \mathbf{K}_{eb}^{i-1} \Delta \mathbf{v}^i + \mathbf{q}_b^{i-1}) = \mathbf{B} \mathbf{T} \quad (30)$$

where $\mathbf{K}_{eb}^{i-1} = \int_0^L \mathbf{B}_b^T(x) k_b^{i-1} \mathbf{B}_b(x) dx$ = contribution of the interface to the element stiffness; and $\mathbf{q}_b^{i-1} = \int_0^L \mathbf{B}_b^T(x) s_b^{i-1}(x) dx$ = contribution of the interface to the element resisting forces. Noting that the boundary terms in (30) can be written as $\delta \mathbf{v}^T \mathbf{P}$, where

\mathbf{P} are the applied nodal forces and taking account of the arbitrary nature of virtual displacements $\delta \mathbf{v}$ simplifies (30) to

$$\mathbf{T}^T \mathbf{q}^i + \mathbf{K}_{eb}^{i-1} \Delta \mathbf{v}^i + \mathbf{q}_b^{i-1} = \mathbf{P} \quad (31)$$

After replacing $\mathbf{q}^i = \mathbf{q}^{i-1} + \Delta \mathbf{q}^i$ in (31) and moving the resisting forces to the right-hand side, the equilibrium equations assume their final form

$$\mathbf{T}^T \Delta \mathbf{q}^i + \mathbf{K}_{eb}^{i-1} \Delta \mathbf{v}^i = \mathbf{P} - \mathbf{q}^{i-1} - \mathbf{q}_b^{i-1} \quad (32)$$

The combination of the compatibility equation in (21) and the equilibrium equation in (32) yields

$$\begin{bmatrix} -\mathbf{F}_e^{i-1} & \mathbf{T} \\ \mathbf{T}^T & \mathbf{K}_{eb}^{i-1} \end{bmatrix} \begin{bmatrix} \Delta \mathbf{q}^i \\ \Delta \mathbf{v}^i \end{bmatrix} = \begin{bmatrix} \mathbf{v}_r^{i-1} \\ \mathbf{P} - \mathbf{q}^{i-1} - \mathbf{q}_b^{i-1} \end{bmatrix} \quad (33)$$

On the right-hand side of (33) are the displacement residuals \mathbf{v}_r^{i-1} from the violation of the compatibility equation at the end of the last Newton-Raphson iteration and the unbalanced forces $\mathbf{P} - \mathbf{q}^{i-1} - \mathbf{q}_b^{i-1}$, which only makes sense in the assembled form at the structural level, because \mathbf{P} cannot be isolated for each element. It should be noted that as the iterative solution converges in each load step, the displacement residuals \mathbf{v}_r^{i-1} reduce to zero in each element, thus satisfying element compatibility. The same is true for the assembled unbalanced forces at the structural level, thus satisfying global equilibrium.

NUMERICAL IMPLEMENTATION OF MIXED FORMULATION

Several alternatives exist for the numerical implementation of the mixed formulation. The most advantageous implementation depends on the computer architecture and the size of structural system. Ayoub and Filippou (1999) discussed alternative implementation strategies for the mixed formulation of an anchored reinforcing bar, which bears a significant resemblance to the composite girder problem. In the following only the direct state determination with condensation of force degrees of freedom in (33) is presented.

Element State Determination with Condensation of Force Degrees of Freedom

The element nodal forces $\Delta \mathbf{q}$ are condensed out of the system of equations in (33)

$$\Delta \mathbf{q}^i = (\mathbf{F}_e^{i-1})^{-1} (\mathbf{T} \Delta \mathbf{v}^i - \mathbf{v}_r^{i-1}) \quad (34)$$

The substitution of $\Delta \mathbf{q}$ from (34) into the second relation of (33) yields

$$\mathbf{T}^T (\mathbf{F}_e^{i-1})^{-1} (\mathbf{T} \Delta \mathbf{v}^i - \mathbf{v}_r^{i-1}) + \mathbf{K}_{eb}^{i-1} \Delta \mathbf{v}^i = \mathbf{P} - \mathbf{q}^{i-1} - \mathbf{q}_b^{i-1} \quad (35)$$

which becomes after collecting terms

$$[\mathbf{T}^T (\mathbf{F}_e^{i-1})^{-1} \mathbf{T} + \mathbf{K}_{eb}^{i-1}] \Delta \mathbf{v}^i = \mathbf{P} - \mathbf{q}^{i-1} - \mathbf{q}_b^{i-1} + \mathbf{T}^T (\mathbf{F}_e^{i-1})^{-1} \mathbf{v}_r^{i-1} \quad (36)$$

Eq. (36) is the element equilibrium equation. Matrix \mathbf{T} accomplishes the transformation of stiffness and resisting forces to the complete set of displacement degrees of freedom \mathbf{v} that include the rigid body modes of the element. After transformation to the global coordinate system, the element equilibrium equations in (36) are assembled for the structural model by imposing displacement compatibility at the nodes. This corresponds to the direct assembly of element stiffness matrices and resisting force vectors according to well-established principles of structural analysis. The global system of equations is solved iteratively by any one of several strategies of which the classical Newton-Raphson method is the best known.

The condensation of force degrees of freedom at the element level results in lack of continuity of internal forces across el-

ement boundaries. This discontinuity can, however, be minimized by appropriate selection of force and displacement interpolation functions, as discussed in the following section. Moreover, Zienkiewicz and Taylor (1989) clearly showed that undesirable oscillations of displacement increments result under excessive continuity requirements and recommended relaxing locally the continuity of the force field. The condensation of force degrees of freedom is, therefore, the superior solution strategy for the system in (33).

Selection of Interpolation Functions and Stability of Mixed Formulation

The order and continuity of force and displacement interpolation functions is very important in a mixed formulation, as certain choices might lead to meaningless results (Zienkiewicz and Taylor 1989). For stability of the formulation, the rank of matrix \mathbf{T} in the expression $\mathbf{T}^T (\mathbf{F}_e^{i-1})^{-1} \mathbf{T}$ should not be larger than the rank of the flexibility matrix for the limit case in which the interface stiffness matrix is zero. For this to be the case the number of unknowns n'_v in vector \mathbf{v} after excluding the rigid body modes should be less or equal to the number of unknowns n_q in vector \mathbf{q} (Ayoub and Filippou 1999)

$$n_q \geq n'_v \quad (37)$$

In the limit case of zero interface stiffness, there are four rigid body modes of the system in Fig. 3, so that $n'_v = 10 - 4 = 6$. With $n_q = 6$ according to Fig. 3, (37) is satisfied. The selection of suitable stress and displacement interpolation functions is further guided by de Veubeke's principle of limitation (1965): there is no accuracy gain by increasing the order of the force field beyond the order of the deformation field that respects the compatibility condition. This is, however, relevant only under linear elastic material behavior, and advantages might accrue from higher order force interpolation functions under nonlinear material behavior.

The simplest selection for the force and displacement interpolation functions within the above constraints and the continuity requirements for the integrals of the terms in (36) is (1) conventional cubic Hermitian polynomials for the transverse displacements and linear polynomials for the bending moment noting that cubic Hermitian polynomials are C^1 continuous across element boundaries, as required by the presence of the second derivative in the differential operator \mathbf{L} ; and (2) quadratic polynomials for the axial displacements and linear polynomials for the axial forces. This selection results in the displacement and force degrees of freedom for the composite element in Fig. 3. The axial displacement degrees of freedom at the internal nodes of the element in Fig. 3(a) are condensed out of the equilibrium equations in (36) before assembly. All force degrees of freedom are condensed out of the system in (33) according to (34). A mixed formulation with higher order force and displacement interpolation functions is also possible but is not pursued in this paper. The trade-off between additional local degrees of freedom and accuracy of local and global element response is, however, worth pursuing in future studies.

MODEL EVALUATION

The ability of the proposed model to simulate the global and local response of steel-concrete girders with partial composite action under monotonic and cyclic loads is evaluated by correlation studies with experimental results and by a comparison of the results of the mixed formulation with the well-known displacement formulation.

McGarraugh-Baldwin Composite Girder

The first correlation study refers to the simply supported beam under third-point loading tested by McGarraugh and

Baldwin (1971). Fig. 4 shows the specimen geometry and load setup. Specimen B4 has a slab width of 72 in. The concrete compressive strength is 4.90 ksi, and the steel yield strength is 35.4 ksi. The force-slip response of the shear connectors was established in push-out tests and was also measured in the actual test. The analyses were conducted with the material models in Fig. 2, except that a bilinear force-slip relation is used for the interface with a yield force of 15 kips at 0.025 in. slip and an ultimate strength of 24 kips at 0.3 in. slip. These values result from a best fit of the bilinear relation to the measured connector response in Fig. 7 of McGarraugh and Baldwin (1971).

Fig. 5 shows the load-displacement response of the composite girder. The analytical results are obtained with the proposed mixed formulation using 4 elements with five-point Gauss-Lobatto integration and with the classical displacement formulation using 4 and 16 elements with 10 degrees of freedom/element, as shown in Fig. 3. Internal degrees of freedom are condensed out in the element for numerical efficiency. The three analytical results are essentially identical and agree quite well with the measured response. Fig. 5 also shows the response of the girder under full and no composite action for comparison. Figs. 6 and 7 show the curvature and bending moment distributions in the composite girder at load point A of Fig. 5. The discrepancies between the mixed formulation and the displacement formulation are rather obvious. The displacement formulation results in discontinuous curvature values at the nodes of the finite-element model, and these discontinuities are rather pronounced. This is even the case with 16 elements. Although the curvature distributions of the mixed model are also discontinuous, the jump in value is very small. The bending moment distribution in Fig. 7 clearly demon-

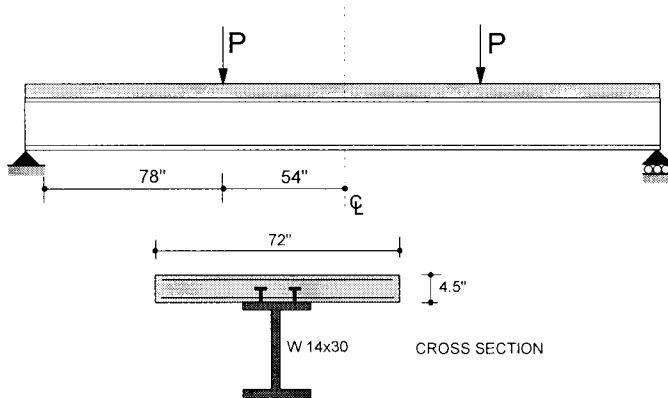


FIG. 4. Composite Girder under Third Span Loading by McGarraugh and Baldwin (1971)

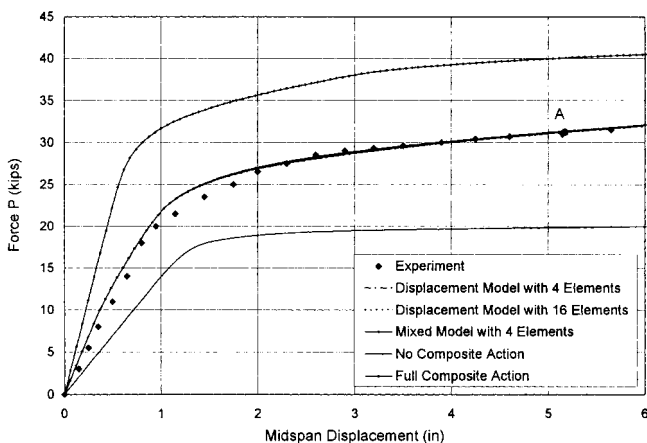


FIG. 5. Load-Displacement Response for McGarraugh-Baldwin Girder

strates the superiority of the mixed formulation, which is able to match the exact moment diagram. It is worth noting that the total resisting moment of the composite girder is linear in the absence of any distributed element loads, irrespective of the shear force transfer at the interface between concrete slab and steel girder. By contrast, even the displacement model with 16 elements exhibits significant jumps in value near the yield front of the beam. The superiority of the mixed formulation in accurately representing the internal force distribution of the girder is even more obvious in Fig. 8, which depicts the axial force distribution in the steel girder. The mixed model with 4 elements is better than the displacement model with 16 elements in representing the smooth variation of axial force, whereas the displacement model with 4 elements exhibits a rather irregular distribution. Finally, Fig. 9 shows the distribution of the relative slip at the interface between steel girder and concrete deck. In this case all analytical results agree rather well but tend to overestimate the measured slip at the connectors near the ends of the beam. It is obvious from the preceding discussion that the mixed formulation combines the advantages of the force formulation with regard to internal force fields with those of the displacement formulation with regard to the approximation of beam displacements and relative slip at the interface of the composite girder.

To illustrate the numerical difficulties that may arise from the rather irregular internal force distributions of the displacement model, the composite girder is reexamined under the condition of a softening connector. The bilinear shear force-slip relation of the connector is now assumed to reach a value of 30 kips at a slip of 0.025 in. and then to drop to an ultimate

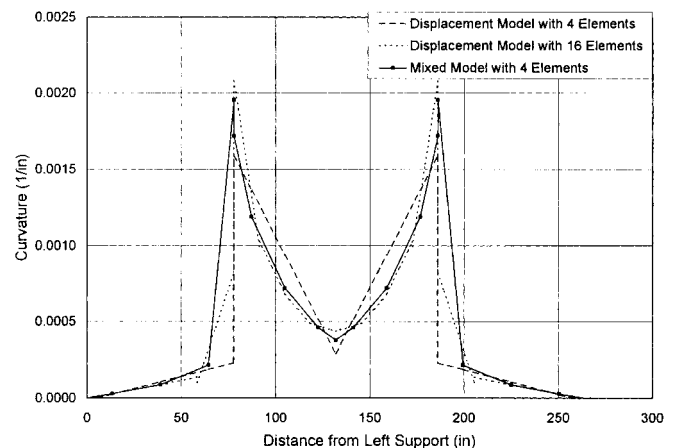


FIG. 6. Curvature Distribution for McGarraugh-Baldwin Girder at Load Point A

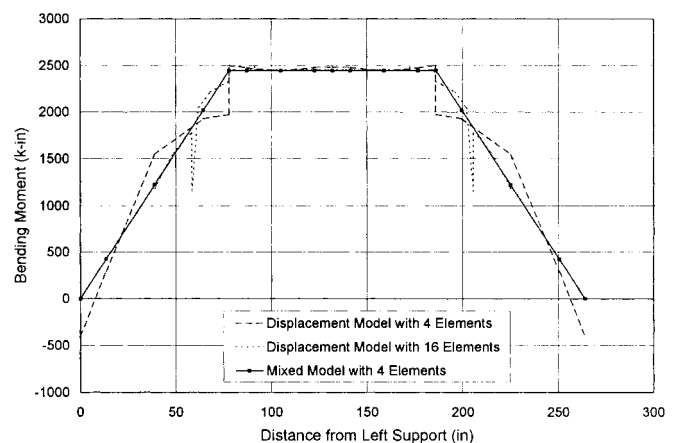


FIG. 7. Bending Moment Distribution for McGarraugh-Baldwin Girder at Load Point A

strength value of 5 kips at 0.30 in. slips. Figs. 10–13 show the global and local response of the composite beam for this case. Fig. 10 shows that numerical instabilities arise in the softening domain of the displacement model with 4 elements, and considerable skill and numerical effort is required to overcome this point and complete the response. No such difficulties were observed with the mixed formulation, which exhibits very robust numerical behavior under softening conditions. The same is more or less true for the displacement model with 16 elements as long as the steel girder itself does not undergo softening, in which case serious numerical instabilities ensue on account of damage localization. The mixed model over-

comes these difficulties with its superior internal force approximation and the resulting coarse finite-element discretization. Figs. 11–13 depict the distribution of axial force, curvature, and bending moment for the softening girder. The irregular nature of the internal force distributions of the displacement model with 4 elements is again pronounced, and the improvement that is achieved by mesh refinement to 16 elements is obvious. The superiority of the mixed model with 4 elements over the displacement model with 16 elements and, therefore, many more internal degrees of freedom, is rather

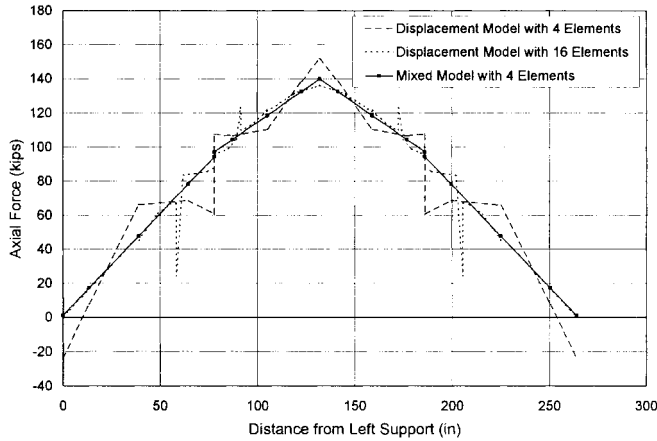


FIG. 8. Axial Force Distribution for McGarraugh-Baldwin Girder at Load Point A

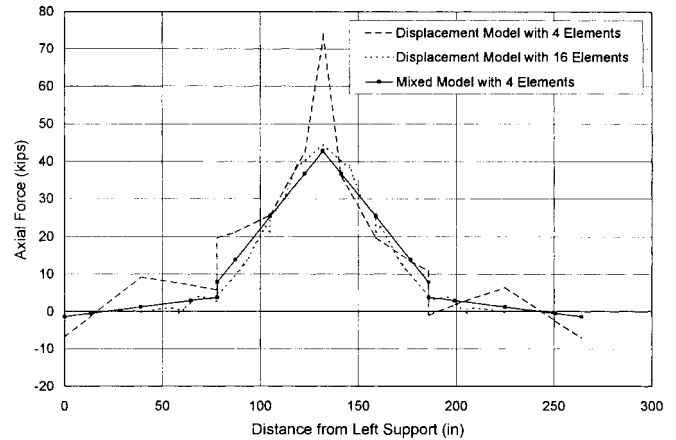


FIG. 11. Axial Force Distribution for Softening Girder at Load Point A

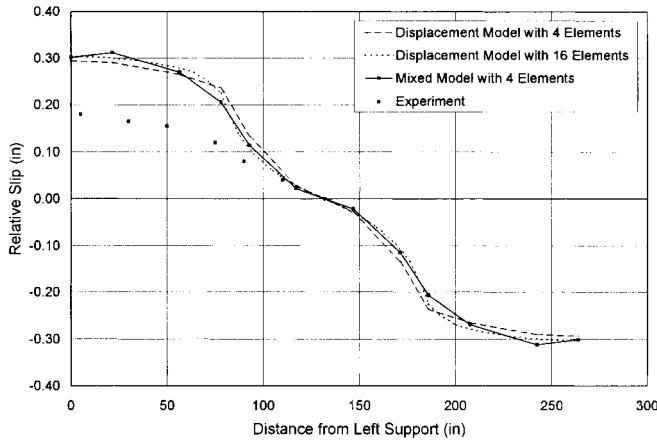


FIG. 9. Slip Distribution for McGarraugh-Baldwin Girder at Load Point A

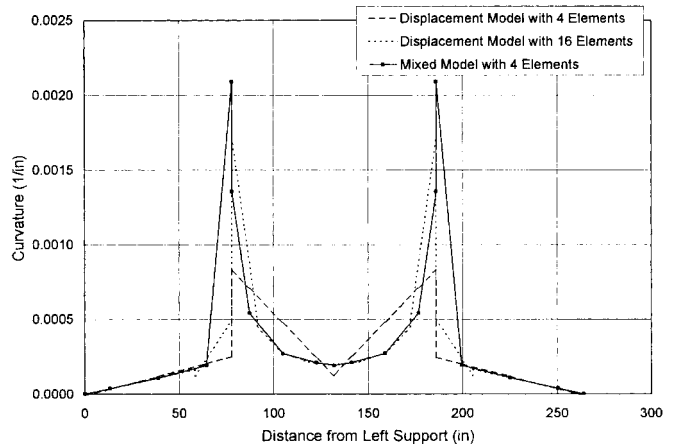


FIG. 12. Curvature Distribution for Softening Girder at Load Point A

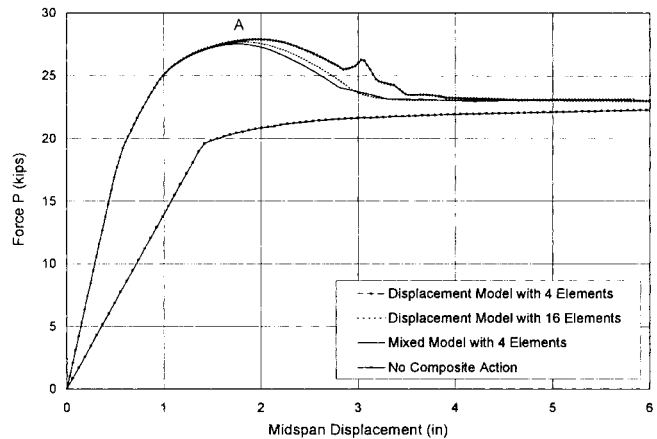


FIG. 10. Load-Displacement Response for Softening Girder

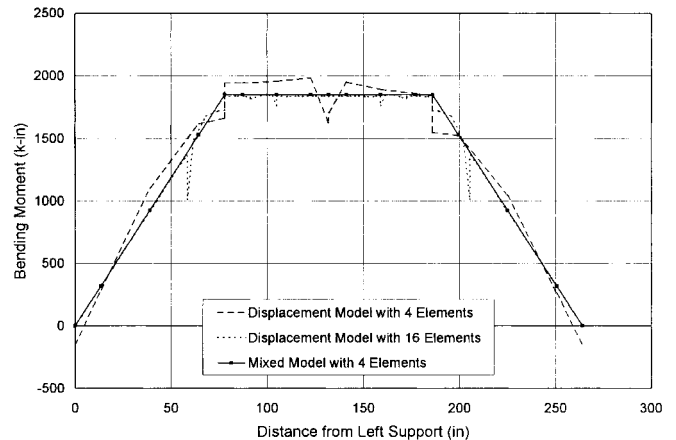


FIG. 13. Bending Moment Distribution for Softening Girder at Load Point A

impressive. It is worth noting the small discontinuities of the axial force distribution at the nodes of the mixed model in Fig. 11 and the more pronounced curvature discontinuities under softening in Fig. 12. It is also worth noting that the strains in the steel girder and concrete deck are considerably underestimated with the displacement model with 4 elements, because the maximum curvature value under the point of load application is only about a third of the value in the mixed model and in the displacement model with 16 elements. Thus, the estimation of local damage with the displacement model requires a fine mesh discretization and increases the cost of the analysis. No such fine mesh discretization is necessary in the mixed formulation for accurate local response. This is an important advantage of the proposed model in the damage assessment of structures under extreme excitations, as it results in considerable savings in the total number of model degrees of freedom.

Bursi and Ballerini Beam-Column Specimen

Bursi and Ballerini (1996) conducted a series of tests to investigate the effect of partial composite action on the hysteretic response of steel-concrete composite girders. After push-pull tests to determine the cyclic load-slip behavior of shear connectors, three tests of a beam-column frame system representative of a composite building structure were performed. The degree of composite action varied from full to low according to the classification criteria of Eurocode 4 ("Design" 1992). The dimensions and loading arrangement of the test frame are shown in Fig. 14(a). The steel girder consists of an IPE 330 section connected to the reinforced concrete

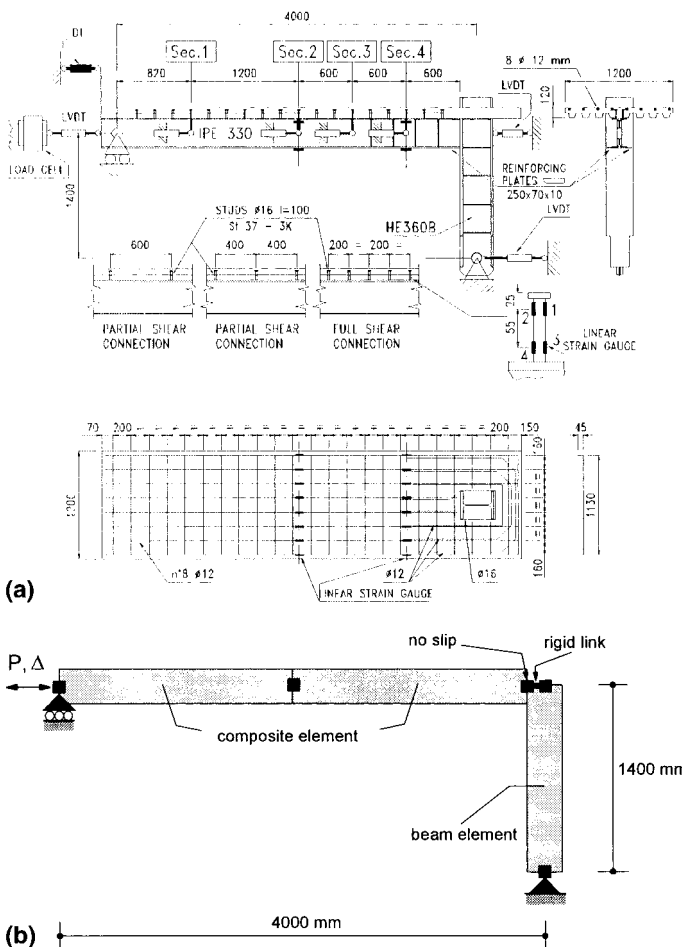


FIG. 14. (a) Bursi and Ballerini Beam-Column Specimen (1996); (b) Model of Bursi and Ballerini Beam-Column Specimen (1996)

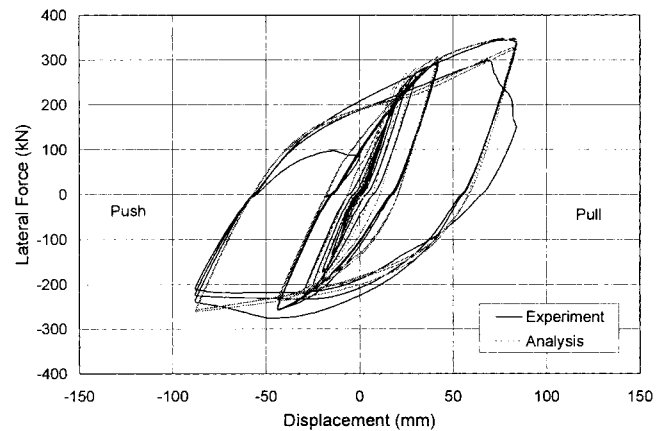


FIG. 15. Global Response for Bursi-Ballerini Specimen with Partial Composite Action

slab by $\varnothing 16$ Nelson studs (St 37-3k) in two rows. The steel column consists of an HE 360B section. At the beam-column joint the concrete slab is cast around the column, and the steel beam is welded to the column flange. The material properties of the test frame are concrete compressive strength $f'_c = 36.8$ MPa, structural steel yield strength $f_y = 329$ MPa, reinforcing steel yield strength $f_y = 482$ MPa, and yield force of shear stud $f_{by} = 65.3$ kN.

The analytical model of the specimen is shown in Fig. 14(b). The column consists of a single beam-column element because it remained elastic during the test. The composite girder is represented by two composite elements. The girder beam is connected to the column by appropriate constraints of displacement degrees of freedom at the respective end nodes of the beam and column element. Because the connection between composite beam and steel column does not allow for connector slip, a constraint on the horizontal degrees of freedom is imposed at the beam-column interface, as shown in Fig. 14(b). The cross section of the steel girder is modeled with 12 fibers, whereas the cross section of the reinforced concrete slab consists of 10 fibers. Five integration points are used for each composite beam element, and the hysteretic shear-force slip relation for the connectors follows the model in Fig. 2(d).

The experimental and analytical load-displacement response of the specimens is compared in Fig. 15 for the case of partial interaction and shows very good agreement. The accuracy and numerical robustness of the proposed model are very satisfactory. Better agreement between analytical and experimental results can be achieved by accounting for residual stresses in the steel girder for the discrepancy in the preyield response, the local buckling of the steel girder at ultimate for the discrepancy in cyclic moment resistance in the "weak" loading direction, and the severe cracking of the concrete slab that leads to relative slip of the reinforcing steel. Such improvements are beyond the scope of the present study. It is remarkable that the model can represent rather well the strength loss in the "strong" loading direction due to cyclic strength deterioration of the connectors.

CONCLUSIONS

This paper presents a new inelastic beam element for the analysis of steel-concrete girders with partial composite action under monotonic and cyclic loads. The element is derived from a two-field mixed formulation with independent approximation of internal forces and transverse displacements. The nonlinear response of the steel and concrete component of the girder is based on the section discretization into fibers with uniaxial hysteretic material models for the constituent mate-

rials. The partial interaction between concrete deck and steel girder through shear connectors is accounted for by an interface model with distributed force transfer characteristics. A direct state determination algorithm for the implementation of the composite element in a general purpose nonlinear analysis program is presented, and the stability characteristics of the algorithm are discussed in conjunction with the selection of appropriate force and displacement interpolation functions.

Numerical correlation studies with the well-known displacement formulation reveal the advantages of the proposed model on account of the accurate approximation of the internal force field in the element. In fact, the total bending moment distribution is always exact irrespective of the presence of shear forces at the interface. At the same time, the mixed formulation permits a more accurate description of the relative displacement at the interface between steel girder and concrete slab than is possible with a pure force formulation. Thus, both internal forces and internal deformations are represented much better than with available displacement-based models. The numerical correlation studies also reveal that the proposed model achieves a specified global and local response accuracy with much fewer elements than displacement-based formulations. This results in reduction of the total number of degrees of freedom in a structural model and in appreciable cost savings of an analytical simulation.

ACKNOWLEDGMENTS

The writers thank Prof. Oreste Bursi of the University of Trento for providing his test data of the composite beam-column specimens and shear connectors. This study was partially supported by subcontract to the University of Nebraska, Lincoln, Nebr., as part of National Science Foundation Grant No. 140-20402 of the U.S.-Japan Program on Composite Structures with Prof. Atorod Azizinamini as principal investigator. This support is gratefully acknowledged. The opinions in the paper are those of the writers and do not reflect the views of the sponsoring agency.

APPENDIX I. REFERENCES

Adekola, A. O. (1968). "Partial interaction between elasticity connected elements of a composite beam." *Int. J. Solids and Struct.*, 4, 1125–1135.

Amadio, C., and Fragiaco, M. (1993). "A finite element model for the study of the creep and shrinkage effects in composite beams with deformable shear connections." *Costruzioni Metalliche*, (4), 213–228.

Ayoub, A., and Filippou, F. C. (1997). "A model for composite steel-concrete girders under cyclic loading." *ASCE Struct. Congr. XV*.

Ayoub, A., and Filippou, F. C. (1999). "Mixed formulation of bond slip problems under cyclic loads." *J. Struct. Engrg.*, ASCE, 125(6), 661–671.

Bursi, O. S., and Ballerini, M. (1996). "Behavior of a steel-concrete composite substructure with full and partial shear connection." *Proc., 11th World Conf. on Earthquake Engrg.*

Ciampi, V., and Carlesimo, L. (1986). "A nonlinear beam element for seismic analysis of structures." *Proc., 8th Eur. Conf. on Earthquake Engrg.*, 6.3/73–6.3/80.

Cosenza, E., and Mazzolani, S. (1993). "Analisi in campo lineare di travi composte con connessioni deformabili: Formule esatte e risoluzioni alla differenza." *1st Indian Workshop on Compos. Struct.*, 1–21.

Daniels, B. J., and Crisinel, M. (1993). "Composite slab behavior and strength analysis. I: Calculation procedure." *J. Struct. Engrg.*, ASCE, 119(1), 16–35.

"Design of composite steel and concrete structures, part 1-1: General rules and rules for buildings." (1992). *Eurocode 4*. European Committee for Standardization, Brussels.

de Veubeke, B. F. (1965). "Displacement and equilibrium models in finite element method." *Stress Analysis*, 145–197.

Eligehausen, R., Popov, E. P., and Bertero, V. V. (1983). "Local bond stress-slip relationships of deformed bars under generalized excitations." *Rep. No. UCB/EERC-83/23*, Earthquake Engrg. Res. Ctr., University of California, Berkeley, Calif.

El-Tawil, S., Sanz-Picon, C. F., and Deierlein, G. G. (1995). "Evaluation of ACI 318 and AISI (LFRD) strength provisions for composite beam-columns." *J. Constructional Steel Res.*, 34, 103–123.

Filippou, F. C., Popov, E. P., and Bertero, V. V. (1983). "Effects of bond

deterioration on hysteretic behavior of reinforced concrete joints." *Rep. No. UCB/EERC-83/19*, Earthquake Engrg. Res. Ctr., University of California, Berkeley, Calif.

Hajjar, J. F., Schiller, P. H., and Molodan, A. (1997). "A distributed plasticity model for concrete-filled steel tube beam-columns with interlayer slip. Part I: Slip formulation and monotonic analysis." *ST 97-1*, University of Minnesota, Minneapolis.

Karsan, I. D., and Jirsa, J. O. (1969). "Behavior of concrete under compressive loadings." *J. Struct. Div.*, ASCE, 95(12), 2543–2563.

McGarraugh, J. B., and Baldwin, J. W. (1971). "Lightweight concrete-steel composite beams." *Engrg. J.*, 8(3), 90–98.

Menegotto, M., and Pinto, P. E. (1973). "Method of analysis for cyclically loaded reinforced concrete plane frames including changes in geometry and non-elastic behavior of elements under combined normal force and bending." *Proc., IABSE Symp. on Resistance and Ultimate Deformability of Struct. Acted on by Well Defined Repeated Loads*, 15–22.

Mirza, S. A., and Skrabek, B. W. (1991). "Reliability of short composite beam-column strength interaction." *J. Struct. Engrg.*, ASCE, 117(8), 2320–2339.

Monti, G., Filippou, F. C., and Spacone, E. (1997). "Finite element for anchored bars under cyclic load reversals." *J. Struct. Engrg.*, ASCE, 123(5), 614–623.

Neuenhofer, A., and Filippou, F. C. (1997). "Evaluation of nonlinear frame finite-element models." *J. Struct. Engrg.*, ASCE, 123(7), 958–966.

Neuenhofer, A., and Filippou, F. C. (1998). "Geometrically nonlinear flexibility-based frame finite element." *J. Struct. Engrg.*, ASCE, 124(6), 704–711.

Newmark, N. M., Siess, C. P., and Viest, I. M. (1951). "Tests and analysis of composite beams with incomplete interaction." *Proc., Soc. for Experimental Stress Analysis*, 9(1).

Robinson, H., and Naraine, K. S. (1988). "Slip and Uplift Effects in Composite Beams." *Engrg. Found. Conf. on Compos. Constr.*

Salari, M. R., Spacone, E., Shing, P. B., and Frangopol, D. (1998). "Non-linear analysis of composite beams with deformable shear connectors." *J. Struct. Engrg.*, ASCE, 124(10), 1148–1158.

Salari, R., Spacone, E., Shing, P. B., and Frangopol, D. M. (1997). "Behavior of composite structures under cyclic loading." *ASCE Struct. Congr. XV*, 731–735.

Scott, B. D., Park, R., and Priestley, M. J. N. (1982). "Stress-strain behavior of concrete confined by overlapping hoops at low and high strain rates." *ACI Struct. J.*, 79(1), 13–27.

Spacone, E., Filippou, F. C., and Taucer, F. F. (1996a). "Fiber beam-column model for nonlinear analysis of RC frames. I: Formulation." *Earthquake Engrg. and Struct. Dyn.*, 25(7), 711–725.

Spacone, E., Filippou, F. C., and Taucer, F. F. (1996b). "Fiber beam-column model for nonlinear analysis of RC frames. II: Applications." *Earthquake Engrg. and Struct. Dyn.*, 25(7), 727–742.

Timoshenko, S. P. (1925). "Analysis of bi-metal thermostats." *J. Opt. Soc. Am.*, 11, 233–255.

Viest, I. M., Colaco, J. P., Furlong, R. W., Griffis, L. G., Leon, R. T., and Wylie, L. A. (1997). *Composite construction: Design for buildings*. Wiley, New York.

Yassin, M. H. M. (1994). "Nonlinear analysis of prestressed concrete structures under monotonic and cyclic loads." PhD thesis, University of California, Berkeley, Calif.

Zienkiewicz, O. C., and Taylor, R. L. (1989). *The finite element method. Volume 1. Basic formulation and linear problems*. McGraw-Hill, London.

Zienkiewicz, O. C., and Taylor, R. L. (1989). *The finite element method. Volume 2. Solid and fluid mechanics, dynamics and non-linearity*. McGraw-Hill, London.

APPENDIX II. NOTATION

The following symbols are used in this paper:

- $\mathbf{a}(x)$ = matrix of displacement interpolation functions;
- $\mathbf{b}(x)$ = vector of force interpolation functions;
- $\mathbf{e}(x)$ = vector of deformations at distance x ;
- $e_b(x)$ = relative slip at interface at distance x ;
- $\mathbf{f}_i(x)$ = section flexibility matrix;
- h_1, h_2 = distance of centroid of concrete and steel component from interface, respectively;
- i = Newton-Raphson iteration number;
- \mathbf{F} = element flexibility matrix;
- \mathbf{K}_b = bond element stiffness matrix;
- M_c, M_s = concrete and steel bending moment, respectively;
- N_c, N_s = concrete and steel axial force, respectively;

n'_v, n_q = order of displacement and force interpolation functions, respectively;
 \mathbf{P} = vector of externally applied loads;
 \mathbf{q} = vector of element forces;
 $\mathbf{s}(x)$ = vector of forces at distance x ;
 $s_b(x)$ = interface shear force per unit length;
 \mathbf{T} = coupling matrix between displacement and internal force degrees of freedom;

$u_{1c}(x), u_{1s}(x)$ = concrete and steel axial displacement, respectively;
 $u_2(x)$ = transverse displacements;
 V_c, V_s = concrete and steel shear force, respectively;
 \mathbf{v} = vector of element displacements;
 w_y = applied external load;
 ϵ_c, ϵ_s = concrete and steel axial strain, respectively; and
 κ = beam curvature.